Peripheral Mechanisms Mediating the Sustained Antidiabetic Action of FGF1 in the Brain

Jarrad M. Scarlett,[1,2] Kenjiro Muta,[1] Jenny M. Brown,[1] Jennifer M. Rojas,[1,3] Miles E. Matsen,[1] Nikhil K. Acharya,[1] Anna Secher,[4] Camilla Ingvorsen,[4] Rasmus Jorgensen,[4] Thomas Høeg-Jensen,[4] Darko Stefanovski,[5] Richard N. Bergman,[6] Francesca Piccinini,[6] Karl J. Kaiyala,[7] Masakazu Shiota,[8] Gregory J. Morton,[1] and Michael W. Schwartz[1]

Diabetes 2019;68:654–664 | https://doi.org/10.2337/db18-0498

We recently reported that in rodent models of type 2 diabetes (T2D), a single intracerebroventricular (icv) injection of fibroblast growth factor 1 (FGF1) induces remission of hyperglycemia that is sustained for weeks. To clarify the peripheral mechanisms underlying this effect, we used the Zucker diabetic fatty *fa/fa* rat model of T2D, which, like human T2D, is characterized by progressive deterioration of pancreatic β-cell function after hyperglycemia onset. We report that although icv FGF1 injection delays the onset of β-cell dysfunction in these animals, it has no effect on either glucose-induced insulin secretion or insulin sensitivity. These observations suggest that FGF1 acts in the brain to stimulate insulin-independent glucose clearance. On the basis of our finding that icv FGF1 treatment increases hepatic glucokinase gene expression, we considered the possibility that increased hepatic glucose uptake (HGU) contributes to the insulin-independent glucose-lowering effect of icv FGF1. Consistent with this possibility, we report that icv FGF1 injection increases liver glucokinase activity by approximately twofold. We conclude that sustained remission of hyperglycemia induced by the central action of FGF1 involves both preservation of β-cell function and stimulation of HGU through increased hepatic glucokinase activity.

Unlike other therapies for type 2 diabetes (T2D), remission of hyperglycemia lasting for weeks or longer can be induced by a single intracerebroventricular (icv) injection of fibroblast growth factor 1 (FGF1) (1). Although this prolonged antidiabetic effect of icv FGF1 was observed in both *ob/ob* mice and Zucker diabetic fatty *fa/fa* (ZDF) rats, it lasted longer (>4 months) in the former than in the latter animals (~4 weeks), potentially owing to the progressive deterioration of β-cell function characteristic of ZDF rats after hyperglycemia onset (2). Because this deterioration does not occur in *ob/ob* mice (on the C57BL/6 background), the ZDF rat model more closely approximates human T2D, which is also characterized by a progressive loss of β-cell function and mass over time (3).

We therefore selected the ZDF model for the current studies, which were undertaken to identify peripheral mechanisms responsible for sustained glucose lowering induced by the central action of FGF1. Our results suggest that in these animals, icv FGF1 injection induces remission of hyperglycemia both by delaying the onset of β-cell failure and by increasing hepatic glucose uptake (HGU) through increased hepatic glucokinase (GCK) activity.

[1]University of Washington Medicine Diabetes Institute, Department of Medicine, University of Washington, Seattle, WA
[2]Gastroenterology and Hepatology, Department of Pediatrics, University of Washington, Seattle, WA
[3]Department of Physiology, Institute for Diabetes, Obesity and Metabolism, Perelman School of Medicine, University of Pennsylvania, Philadelphia, PA
[4]Novo Nordisk A/S, Måløv, Denmark
[5]New Bolton Center, School of Veterinary Medicine, University of Pennsylvania, Philadelphia, PA
[6]Diabetes and Obesity Research Institute, Cedars-Sinai Medical Center, Los Angeles, CA
[7]Department of Oral Health Sciences, School of Dentistry, University of Washington, Seattle, WA
[8]Department of Molecular Physiology and Biophysics, Vanderbilt University School of Medicine, Nashville, TN

Corresponding author: Michael W. Schwartz, mschwart@u.washington.edu

Received 3 May 2018 and accepted 29 October 2018

This article contains Supplementary Data online at http://diabetes.diabetesjournals.org/lookup/suppl/doi:10.2337/db18-0498/-/DC1.

See accompanying article, p. 476.

RESEARCH DESIGN AND METHODS

Animals

All procedures were performed in accordance with the National Institutes of Health Guide for the Care and Use of Laboratory Animals and were approved by the institutional animal care and use committee at the University of Washington. Animals were individually housed under specific-pathogen–free conditions in a temperature-controlled room with a 12:12-h light:dark cycle and provided with ad libitum access to water and Purina 5008 chow (Animal Specialties, Inc.). Six-week-old male ZDF rats (ZDF-*Lepr*^{fa}/Crl) and lean controls (ZDL-Lean fa/+) were purchased from Charles River Laboratories and studied once their blood glucose (BG) levels exceeded 250 mg/dL (age ~8 weeks). Study groups were matched for age, body weight (BW), and BG levels.

Surgery

Rats underwent surgical implantation of an indwelling lateral ventricle cannula as previously described (1). Both the carotid artery and the internal jugular vein were cannulated during the same surgical session using established methods (4). Animals were allowed to recover for 7 days before study. Animals whose food intake (FI), BW, or BG had not returned to baseline 7 days after surgery were excluded.

icv Injections

Animals received a single icv injection of either saline vehicle (Veh) or recombinant rat FGF1 (FGF1; ProSpecTany TechnoGene Ltd.), which was dissolved in sterile water at a concentration of 1 μg/μL and injected over 60 s in a volume of 3 μL (total dose 3.0 μg).

Frequently Sampled Intravenous Glucose Tolerance Test

Blood sampling was performed through an arterial catheter in unrestrained, conscious animals as previously described (1,5). After a 5-h fast, baseline fasting blood samples were drawn at −10 and 0 min. After a bolus of 50% dextrose (1 g/kg BW) was injected intravenously (iv) over a period of 15 s, blood (20 μL) was sampled for serial measurement of glucose using a GM9D Analox analyzer (Analox Instruments Ltd.) and for subsequent assay of plasma insulin and lactate levels.

Minimal Model Analysis and Calculations

Plasma insulin and BG profiles during each frequently sampled intravenous glucose tolerance test (FSIGT) were analyzed using MinMod software to quantify insulin-independent glucose disposal (referred to as glucose effectiveness [GE] [S_G]) and insulin sensitivity (S_I) as previously described (1,5) and recently validated in rats (6). The acute insulin response to glucose (AIR_G) was calculated as the mean increment above basal insulin values measured between t = 0 and 4 min. Glucose tolerance was estimated from the incremental area under the glucose curve (AUCglucose) during the FSIGT.

Lactate Kinetics and Hepatic GCK Activity Calculations

Modeled liver GCK activity (K_{GK}), glycolysis, and whole-body lactate clearance were estimated by analyzing the kinetic relationship between plasma glucose and lactate levels obtained during the FSIGT as previously described (7). Because of the reduced sampling number taken in rodents, glycolysis was fixed to a standard value, rather than estimated, to facilitate the parameter estimation.

Direct measurement of liver GCK activity was performed on liver samples that were immediately frozen in liquid nitrogen and subsequently homogenized in 50 mmol/L HEPES, 100 mmol/L KCl, 1 mmol/L EDTA, 5 mmol/L $MgCl_2$, and 2.5 mmol/L dithioerythritol (8). GCK activity was measured in the supernatant fraction after centrifugation as previously described (8).

Intravenous Insulin Tolerance Test

After a 1-week recovery from the FSIGT study, ZDF rats fasted for 5 h underwent an intravenous insulin tolerance test (IVITT). Baseline blood samples and glucometer readings were taken at 0 min, after which animals received an iv bolus of recombinant rat insulin 2 (0.75 units/kg BW) (Novo Nordisk A/S). Blood samples were taken through the arterial catheter at 0, 15, 30, 45, 60, 120, and 180 min for measurement of glucose using a handheld glucometer. The extent of insulin-induced glucose lowering was taken as a measure of whole-body S_I.

Euglycemic Clamp

Two weeks after icv FGF1 injection (3 μg) or Veh (when BG levels were much lower in the former than in the latter group), ZDF rats bearing catheters in the right-side jugular vein and left-side carotid artery were subjected to a variable insulin and glucose infusion protocol designed to ascertain the level of plasma insulin in Veh-treated ZDF rats required to match and maintain BG levels to those of icv FGF1–treated ZDF rats. After a 5-h fast, baseline blood samples and glucometer readings were taken at −10 and 0 min, and beginning at t = 0 min, infusions of both recombinant rat insulin (mU/kg/min; rat insulin 2 synthesized and provided by Novo Nordisk A/S [Supplementary Data]) and glucose (50% dextrose) (mg/kg/min) were initiated simultaneously with rates adjusted to clamp BG levels at 170 mg/dL in both icv Veh- and FGF1-treated rats. Rat insulin was selected for these studies to ensure that endogenous and infused insulin would be detected in equimolar amounts using a rat insulin ELISA. Blood samples were taken at 10-min intervals for a duration of 120 min.

Quantitation of β-Cell Mass

Pancreata were fixed in 10% neutral buffered formalin for 24 h, processed in paraffin, and analyzed as previously described (9). Paraffin blocks were cut into 3-μm sections and stained with guinea pig anti-insulin (Dako) and rabbit anti-Nkx6.1 antibodies (Sigma-Aldrich). Insulin immunoreactivity was visualized with goat anti-guinea pig (Invitrogen) secondary antibody and donkey anti-goat Alexa

Fluor 488 (The Jackson Laboratory). Nkx6.1 immunoreactivity was used to identify β-cells and visualized with donkey anti-rabbit biotin (The Jackson Laboratory), streptavidin horseradish peroxidase (PerkinElmer), and TSA Plus Cyanine 3 (Invitrogen). The slides were counterstained with DAPI to detect cell nuclei and scanned on a VS120 slide scanner at 10× magnification (Olympus), and pancreatic β-cell mass was quantified using Visiomorph software (Visiopharm).

Blood Collection and Tissue Processing

Daily BG levels were measured using a handheld glucometer on blood obtained from tail capillary samples. At study completion, whole-blood samples for plasma hormone measurement were collected into appropriately treated tubes (10), separated into plasma, aliquoted, and stored at −80°C. Plasma insulin (Crystal Chem), corticosterone (Cort) (Crystal Chem), and glucagon (Mercodia) levels were measured by ELISA. Plasma lactate levels were measured using a GM9D analyzer. Plasma lipids were measured with enzymatic colorimetric assays using a triglyceride (TG) kit (Raichem) and nonesterified free fatty acid (FFA) kit (Wako Diagnostics).

Real-time PCR

Total RNA was extracted from liver using TRI Reagent (Sigma-Aldrich) and NucleoSpin RNA (Thermo Fisher Scientific). Levels of specific transcripts for *Gck*, *Pklr*, *Gys2*, *Pck1*, and *G6p* were quantified by real-time PCR (ABI Prism 7900HT; Applied Biosystems) using SYBR Green (Applied Biosystems), and results were normalized to the housekeeping gene 18s. For comparative analysis, RNA ratios of the treatment group were normalized to the icv Veh control group.

Statistical Analysis

All results are expressed as mean ± SEM. Group-by-time designs were analyzed using linear mixed model analysis (SPSS version 23; IBM Corporation, Armonk, NY) and mixed factorial analyses (GraphPad Software, La Jolla, CA) or two-way ANOVA with repeated measures (mixed model) with Bonferroni posttest comparison. For pairs of data, a two-sample unpaired Student *t* test was used. In all instances, $P < 0.05$ was considered significant.

RESULTS

Effect of icv FGF1 on Levels of BG, FI, and BW in ZDF Rats

As expected (11), male ZDF rats fed ad libitum developed hyperglycemia (Fig. 1*A*) between age 7 and 10 weeks. After a single icv injection of FGF1 (3 μg), morning BG levels dropped into the normal range (Fig. 1*A*) for ∼30 days, after which hyperglycemia relapsed (Fig. 1*A*). FI also was reduced transiently (Fig. 1*B*), and although BW was decreased as well, the effect did not achieve statistical significance (Fig. 1*C*). In nondiabetic ZDL controls, FI also was reduced transiently after icv FGF1 injection, but BG levels remained unchanged (Fig. 1*D* and *E*), as is observed in wild-type mice (1).

To assess the contribution made by reduced FI to the glucose-lowering effect of icv FGF1, we performed an additional study in which icv Veh–treated ZDF rats were pair fed to the intake of ZDF rats receiving icv FGF1. Although BG values initially declined in pair-fed controls, as expected (11,12), the effect was transient such that BG levels returned to baseline by day 13 (Fig. 2*A*), concurrent with the restoration of baseline levels of FI and BW (Fig. 2*B* and *C*).

Effect of icv FGF1 Injection on Hormonal and Metabolic Parameters in ZDF Rats

In animals receiving icv Veh, basal plasma insulin levels peaked at the onset of hyperglycemia followed by a progressive decline (Fig. 3*A*), as previously reported (11). In icv FGF1–treated ZDF rats, by comparison, insulin remained at pretreatment levels for 3–4 weeks, followed by a precipitous decline (Fig. 3*A*) that corresponded temporally with hyperglycemia relapse (Fig. 1*A*). Thus, the progressive decline of pancreatic β-cell function characteristic of the ZDF rat model was delayed by ∼3–4 weeks after icv FGF1 injection, and it was during this interval that hyperglycemia was ameliorated. Although plasma glucagon levels were reduced 1 week after icv FGF1 injection, subsequent values did not differ significantly from those of icv Veh–treated controls (Fig. 3*B*). Circulating FFA levels were slightly increased beginning 6 weeks after icv FGF1 injection, but no changes in TG levels were detected (Fig. 3*C* and *D*).

Effect of icv FGF1 Injection on β-Cell Mass

Histochemical analysis of pancreatic islets from icv FGF1– and icv Veh–treated animals (Fig. 4*A*–*C*) revealed a strong association between islet β-cell mass and basal plasma insulin levels. At the 3-week time point after icv injection (when baseline plasma insulin levels were higher in icv FGF1– than icv Veh–treated animals [Fig. 3*A*]), β-cell mass was significantly increased in icv FGF1–treated animals relative to baseline (day 0) and to icv Veh–treated animals at the same 3-week time point. However, this effect was transient such that by week 7 after icv injection, β-cell mass had decreased by 86% to achieve values comparable to those of icv Veh–treated animals (Fig. 4*D*), with plasma insulin levels showing a similar drop (Fig. 3*A*) and BG levels returning to the diabetic range (Fig. 1*A*). These findings suggest that icv FGF1 injection delays the onset of β-cell decompensation in ZDF rats, with the eventual loss of β-cell function then driving diabetes relapse.

Effect of icv FGF1 on the Determinants of Glucose Tolerance in ZDF Rats

To determine the contribution made by the three major determinants of glucose tolerance (insulin secretion, S_I, and GE) to the response to icv FGF1, we performed an FSIGT on a separate cohort of ZDF rats 2 weeks after icv injection of either FGF1 (3 μg) or Veh. At this time point, levels of FI and BW were comparable between groups (Fig. 1*A*–*C*), and by design, fasting BG levels were much lower in icv FGF1– than icv Veh–treated animals (Fig. 5*A*). BG levels

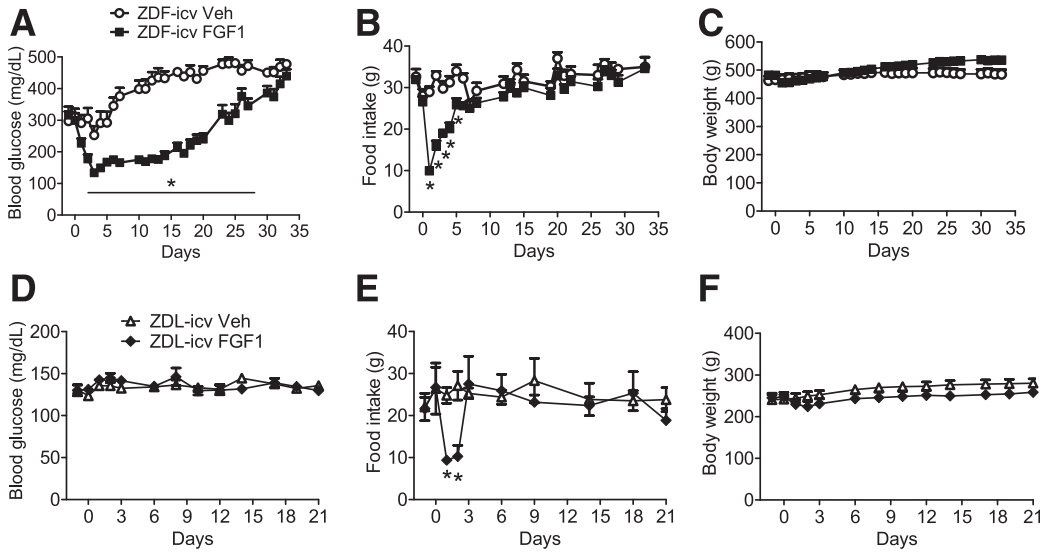

Figure 1—Glucose-lowering effect of a single icv FGF1 injection in ZDF and ZDL rats. Daily BG (*A*), FI (*B*), and BW (*C*) values from ad libitum–fed ZDF rats after a single icv injection of either Veh ($n = 9$) or FGF1 (3 μg; $n = 9$). Daily BG (*D*), FI (*E*), and BW (*F*) values from ad libitum–fed ZDL rats after a single icv injection of either Veh ($n = 7$) or FGF1 (3 μg; $n = 8$). Data are mean ± SEM. *$P < 0.05$ vs. icv Veh.

remained lower in icv FGF1– than icv Veh–treated animals for the duration of the FSIGT, but after correcting for the difference in basal glucose levels, the AUCglucose did not differ significantly between groups (Fig. 5*B* and *C*). In ZDF rats, therefore, treatment with icv FGF1 has no effect on glucose tolerance at a time when basal glucose levels are completely normalized, which agrees with our findings in *ob/ob* mice (1).

As plasma insulin levels declined during the first few weeks after icv injection in Veh-treated animals, but not in those receiving icv FGF1 (Fig. 3*A*), we expected fasting plasma insulin levels to be higher in FGF1-treated animals on day 14 after icv injection before the FSIGT (despite lower BG levels), and this proved to be the case (Fig. 5*D*). After controlling for differences in the basal insulin level, however, no difference was found in AIR_G between groups (Fig. 5*E*, *F*, and *H*). Furthermore, although a trend toward increased S_G was detected in animals receiving icv FGF1 treatment, S_G also did not achieve statistical significance (Fig. 5*G*). Paradoxically, S_I was decreased by ~50% in FGF1-treated animals, although this effect did not reach statistical significance (Fig. 5*I*). Thus, neither glucose-induced insulin secretion nor S_I appear to be affected by icv FGF1 administration.

To further characterize the effect of icv FGF1 on S_I in these animals, we performed an IVITT 1 week after the FSIGT in the same cohort of animals. Because this study demonstrates directly that the glucose-lowering effect of iv insulin injection was in fact reduced in ZDF rats that received icv FGF1 versus icv Veh (Fig. 5*J* and *K*), the antidiabetic action of FGF1 in the brain cannot be attributed to an increase of S_I.

Contribution of Preserved Basal Plasma Insulin Secretion to the Antidiabetic Effect of icv FGF1

To quantify the contribution made by preservation of β-cell function to remission of hyperglycemia induced by icv FGF1, we used a modified glucose clamp protocol

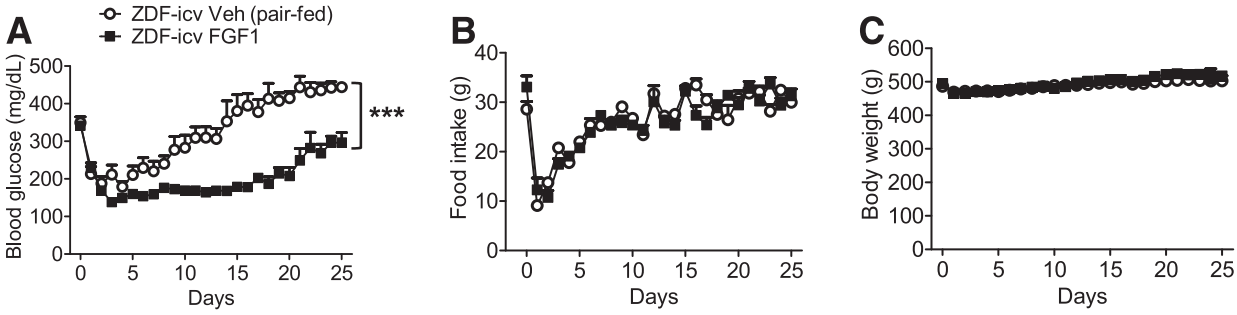

Figure 2—Contribution of transient anorexia to the glucose-lowering effect of icv FGF1 in ZDF rats. Daily BG (*A*), FI (*B*), and BW (*C*) values from pair-fed ZDF rats after a single icv injection of either Veh ($n = 9$) or FGF1 (3 μg; $n = 9$). Data are mean ± SEM. ***$P < 0.001$ vs. icv Veh.

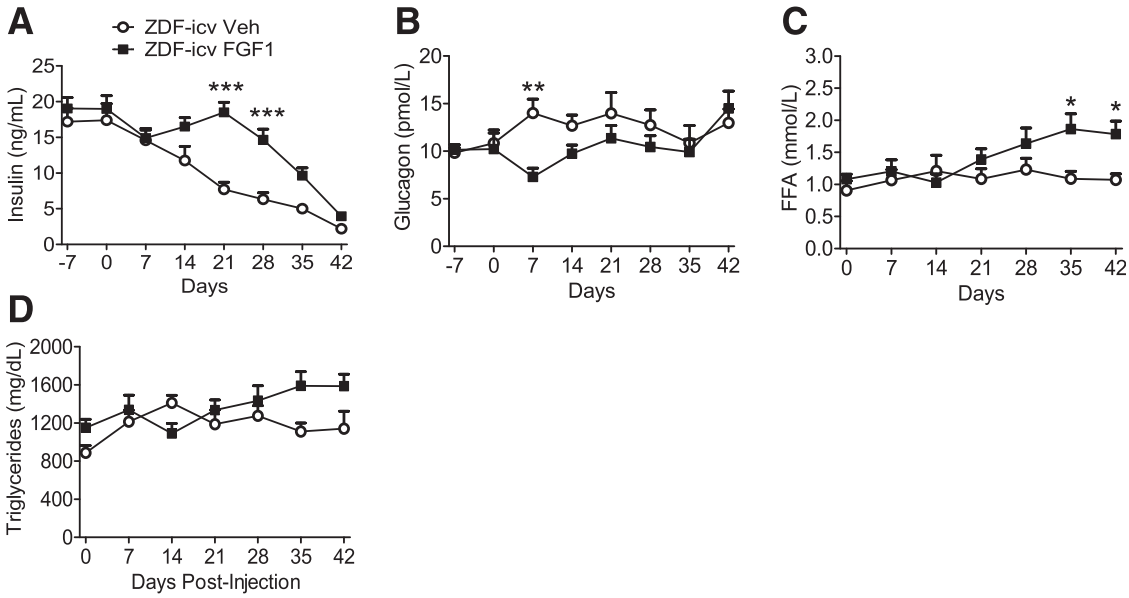

Figure 3—Preserved basal insulin secretion by icv FGF1 in ZDF rats. Weekly plasma insulin (*A*), glucagon (*B*), FFA (*C*), and TG (*D*) from ad libitum–fed ZDF rats after a single icv injection of either Veh ($n = 9$) or FGF1 (3 μg; $n = 9$). Data are mean ± SEM. *$P < 0.05$, **$P < 0.01$, ***$P < 0.001$ vs. icv Veh.

whereby icv Veh–treated ZDF rats received iv insulin at a variable rate designed to reduce their BG level into the normal range, at the same level (170 mg/dL) maintained by ZDF rats treated with icv FGF1 2 weeks earlier (Fig. 6*A*). No difference of FI or BW was found between groups (Fig. 6*B* and *C*), and baseline ($t = 0$ min) plasma BG levels were higher and insulin levels lower in icv Veh– versus icv FGF1–treated animals (Fig. 6*D* and *E*), as expected. After variable-rate iv insulin infusion for ∼70 min (Fig. 6*F*), BG levels were effectively matched between the two groups

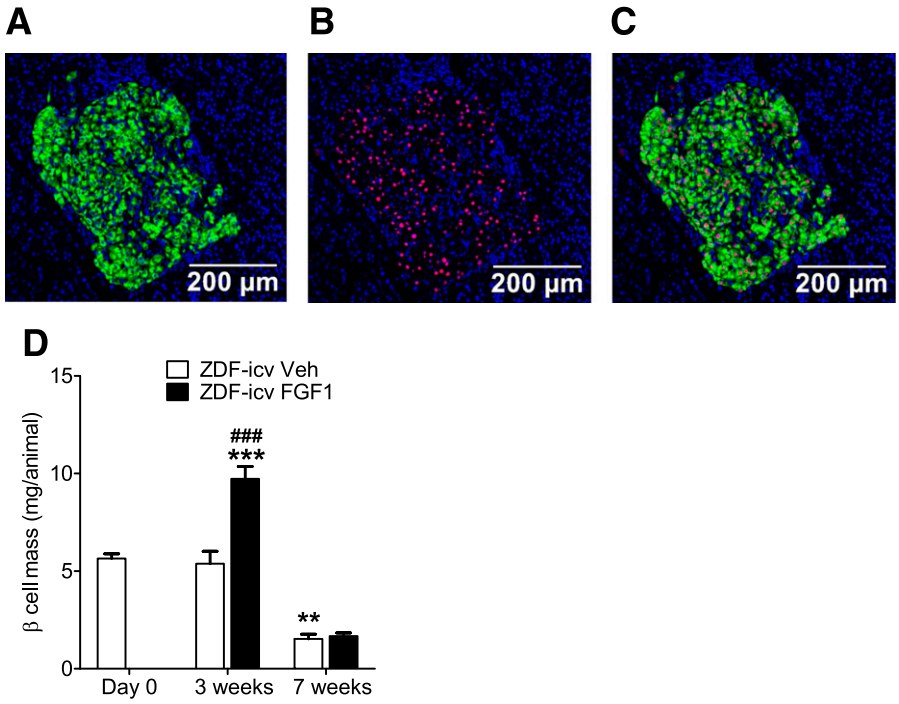

Figure 4—Time course of the effect of icv FGF1 on β-cell mass in ZDF rats. Representative images of staining of pancreatic islet sections from ZDF rats for insulin (*A*), Nkx6.1 (*B*), and merged images (*C*). Pancreatic β-cell mass at day 0 ($n = 7$), 3 weeks ($n = 8$ icv Veh vs. $n = 10$ icv FGF1), and 7 weeks ($n = 9$/group) in ad libitum–fed ZDF rats after a single icv injection of either Veh or FGF1 (3 μg) (*D*). Data are mean ± SEM. **$P < 0.01$ vs. icv Veh at day 0 and 3 weeks; ***$P < 0.001$ vs. icv Veh at day 0, 3 weeks, and 7 weeks; ###$P < 0.001$ vs. icv FGF1 at 7 weeks.

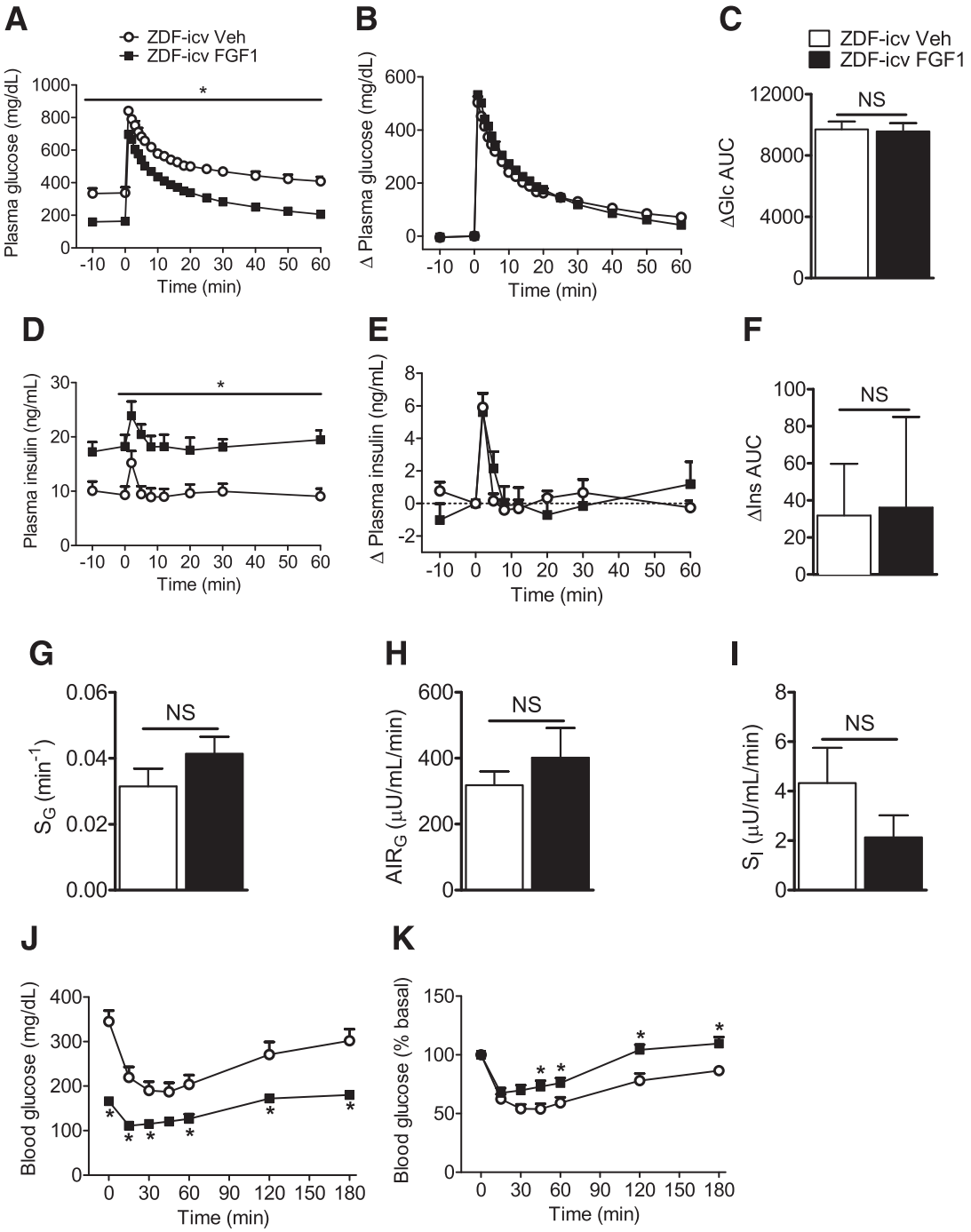

Figure 5—Effect of icv FGF1 on determinants of glucose tolerance in ZDF rats. Plasma glucose (*A*), Δ plasma glucose (correcting for differences in basal glucose) (*B*), Δ plasma AUCglucose (Glc AUC) (*C*), plasma insulin (*D*), Δ plasma insulin (correcting for differences in basal insulin) (*E*), Δ plasma insulin AUC (Ins AUC) (*F*), S_G (*G*), AIR_G (*H*), and S_I (*I*) during an FSIGT in ZDF rats 2 weeks after receiving a single icv injection of either Veh ($n = 7$) or FGF1 (3 μg; $n = 7$). BG (*J*) and percent Δ BG (*K*) during an IVITT in ZDF rats 3 weeks after receiving a single icv injection of either Veh ($n = 7$) or FGF1 (3 μg; $n = 6$). Data are mean ± SEM. *$P < 0.05$ vs. icv Veh.

and remained so for the duration of the study (until t = 120 min) (Fig. 6*D*).

Overall, the plasma insulin level required for icv Veh–treated animals to achieve normoglycemia was approximately twofold greater (Fig. 6*E*) than was observed in icv FGF1–treated animals that spontaneously maintained the same BG level (Fig. 6*D*). This finding is made more striking by the fact that FGF1-treated animals required a variable-rate glucose infusion to prevent their BG from dropping below basal levels (Fig. 6*G*). At baseline, plasma glucagon levels were higher in icv Veh– than in icv FGF1–treated rats (Fig. 6*H*), but there were no differences in plasma Cort

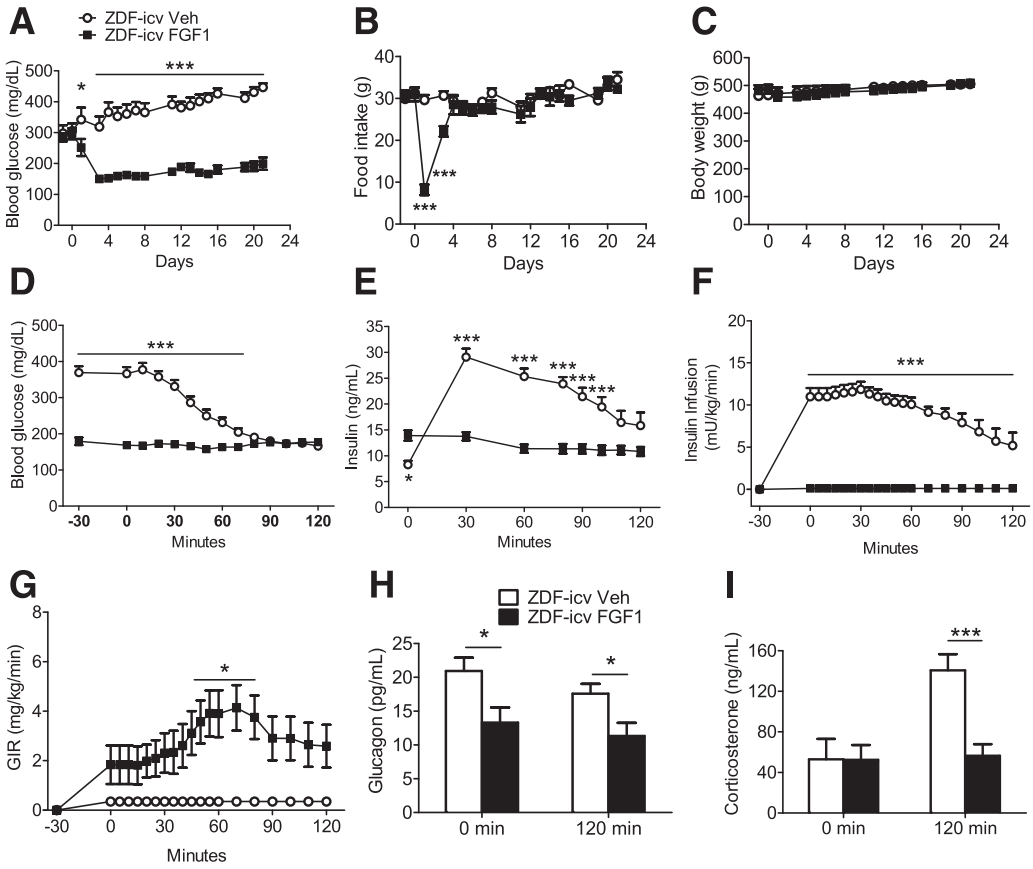

Figure 6— Dependence of basal insulin secretion on antidiabetic effect of icv FGF1. ZDF rats underwent matched euglycemic clamp 14 days after a single icv injection of either Veh ($n = 11$) or FGF1 (3 μg; $n = 11$). Daily morning BG (*A*), FI (*B*), and BW (*C*) values from ad libitum–fed ZDF rats. Plasma glucose (*D*), plasma insulin (*E*), insulin infusion rate (*F*), and glucose infusion rate (GIR) (*G*) during the matched euglycemic clamp. Plasma glucagon (*H*) and plasma Cort (*I*) at the start ($t = 0$ min) and end ($t = 120$ min) of the matched euglycemic clamp. Data are mean ± SEM. $^*P < 0.05$, $^{***}P < 0.001$ vs. icv Veh.

levels (Fig. 6*I*). During the insulin infusion period, plasma glucagon levels remained stable (Fig. 6*H*), whereas plasma Cort levels increased by more than twofold in response to normalization of BG among icv Veh–treated animals (Fig. 6*D*), whereas it did not change in icv FGF1–treated animals (Fig. 6*I*).

Collectively, these data suggest that although a relative increase of basal insulin secretion may contribute, basal insulin cannot fully account for icv FGF1–induced glucose lowering; furthermore, there is no evidence that this effect involves an increase of S_I. Also of note, on the basis of the plasma Cort response, acute normalization of BG levels appears to elicit a stress response in diabetic icv Veh–treated ZDF rats, an effect that is not observed in animals with diabetes remission induced by icv FGF1 injection.

Effect of icv FGF1 Injection on Plasma Lactate and Hepatic GCK Expression and Activity

These considerations collectively suggest that an insulin-independent process must contribute to FGF1-induced remission of hyperglycemia. To test this hypothesis, we focused on HGU, a process that is largely insulin independent, is crucial for normal glucose homeostasis, and is regulated in part by the brain (13,14). Specifically, we investigated whether the mechanism underlying glucose lowering induced by icv FGF1 involves increased hepatic GCK activity, which constitutes a key rate-limiting step for HGU by phosphorylating glucose upon entry into the hepatocyte.

As an initial test of this hypothesis, we considered that the magnitude of the rise of plasma lactate levels in response to a glucose load (which reflects glucose taken up by the liver and subsequently converted by glycolysis to lactate, which is released back into circulation) can be used to estimate hepatic GCK activity in vivo (7,15). To this end, we performed serial measures of plasma lactate levels obtained before and during the previously described FSIGT performed 2 weeks after icv injection of either Veh or FGF1 (Fig. 5). We found that although basal plasma lactate levels were higher in icv Veh– than icv FGF1–treated ZDF rats (Fig. 7*A*), reflecting their much higher basal glucose level, the plasma lactate response to an iv glucose challenge was increased by more than twofold in the FGF1-treated group (Fig. 7*B* and *C*). Model-based estimation of the hepatic K_{GK} from this lactate response (7) demonstrated a similar, more than twofold increase in icv FGF1–treated rats

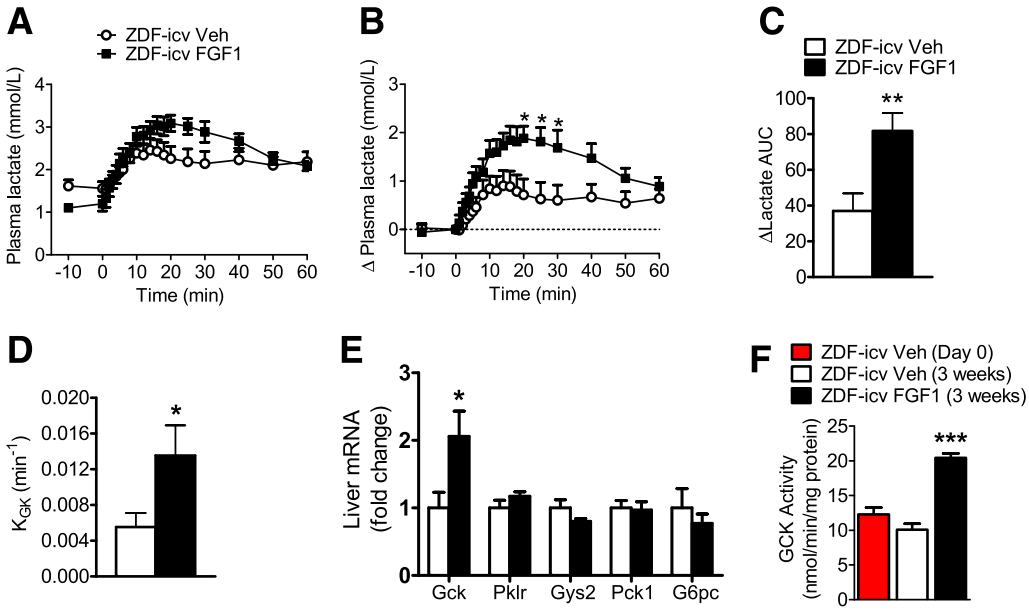

Figure 7—Effect of icv FGF1 on plasma lactate and hepatic GCK in ZDF rats. Plasma lactate (*A*), Δ plasma lactate (correcting for differences in basal lactate) (*B*), Δ plasma lactate AUC (*C*), and calculated hepatic K_{GK} (*D*) during an FSIGT in ZDF rats 2 weeks after receiving a single icv injection of either Veh ($n = 7$) or FGF1 (3 μg; $n = 7$). *E*: Hepatic mRNA expression of *Gck*, *Pklr*, *Gys2*, *Pck1*, and *G6pc* by real-time PCR in ZDF rats 3 weeks after receiving a single icv injection of either Veh ($n = 11$) or FGF1 (3 μg; $n = 11$). *F*: Hepatic GCK activity in ZDF rats at day 0 baseline (icv Veh, $n = 6$) or 3 weeks after receiving a single icv injection of either Veh ($n = 8$) or FGF1 (3 μg; $n = 11$). Data are mean ± SEM. $^*P < 0.05$, $^{**}P < 0.01$, $^{***}P < 0.001$ vs. icv Veh.

relative to icv Veh–treated controls, a highly significant effect (Fig. 7*D*). Model-derived estimates of K_{GK} were well identified, with mean normalized root square error values of 15% (SD 6%) for icv Veh and 11% (SD 5%) for icv FGF1. These data, combined with our biochemical findings of a twofold increase in the expression of both *Gck* mRNA and K_{GK} in the liver of ZDF rats treated with icv FGF1, confirm and validate our model-based finding and offer direct evidence implicating the action of FGF1 in the brain to increase liver GCK activity in the associated remission of hyperglycemia (Fig. 7*E*).

DISCUSSION

We report that in the ZDF rat model of T2D, icv FGF1 injection delays the onset of progressive β-cell dysfunction, and we interpret this finding to suggest that FGF1 action in the brain transiently suppresses pathogenic processes that drive β-cell loss in this model. However, this mechanism alone is unlikely to explain the observed normalization of glycemia because basal plasma insulin levels never increased over pretreatment values in animals receiving icv FGF1 injection. Instead, the rapid decline of plasma insulin levels observed in icv Veh–treated animals was transiently prevented by icv FGF1 injection over a time course that corresponds to the period of diabetes remission. With respect to other peripheral mechanisms of glucose lowering, we observed no effect of icv FGF1 on glucose tolerance, whole-body S_I, or glucose-stimulated insulin secretion; furthermore, circulating levels of Cort, FFAs, or TGs were not altered. Instead, our data point to an action of FGF1 in the brain to increase basal glucose clearance through a mechanism involving increased hepatic GCK activity.

These findings extend previous evidence that the activity of glucoregulatory neurocircuits (16–18) is sensitive to input from FGF peptides, such as FGF19 and FGF21. Although glucose lowering elicited by these peptides was initially hypothesized to involve actions primarily on peripheral tissues (19–21), subsequent work revealed that an action in the brain is sufficient (5,22–26) and may be necessary (27) for this effect. Although the prolonged duration of glucose lowering induced by FGF1 action in the brain is unique (1), the duration of this effect is considerably shorter in ZDF rats than is reported in *ob/ob* mice (1), potentially owing to rapid loss of β-cell mass and function in the former (2), but not the latter, animals (28). Combined with evidence that in our hands, icv FGF1 injection does not induce glucose lowering in rodents with uncontrolled insulin-deficient diabetes (1,29), we interpret these data to suggest that an intact insulin signal is required for the antidiabetic response induced by central administration of FGF1. Consistent with this hypothesis, the observed delay in onset of β-cell dysfunction corresponds closely with the period of diabetes remission induced by icv FGF1 in ZDF rats such that diabetes relapse was accompanied by precipitous declines of both plasma insulin and β-cell mass. In the ZDF rat model, therefore, eventual relapse of hyperglycemia after icv FGF1 injection appears to be driven by the onset of severe, progressive β-cell dysfunction, an effect that does not occur in *ob/ob* mice.

Increased β-cell mass is an integral feature of the adaptation to insulin resistance in ZDF rats. At 5–7 weeks of age, β-cell mass in male ZDF rats is approximately twice that of age-matched ZDL controls, and this expansion continues until 10–12 weeks of age, after which it progressively and markedly declines (30,31). Several potential explanations can be considered for how β-cell mass and function are preserved, albeit transiently, after central administration of FGF1. One obvious possibility is that FGF1 activates neurocircuits that directly control islet function. This hypothesis is consistent with evidence that the pancreas is richly innervated by autonomic fibers (32,33) and that both parasympathetic and sympathetic outflow to the pancreas can powerfully influence not only β-cell function but also, if sustained, islet mass (34,35). Furthermore, retrograde mapping studies reveal that some of the same hypothalamic areas that respond to FGF1 (36) are anatomically linked to efferent circuits innervating pancreatic islets (36), and both β-cell mass and function can be altered by either surgical (37) or pharmacological (38,39) manipulation of these circuits. This explanation is also consistent with the increase of β-cell mass over baseline that was observed 3 weeks after icv FGF1 injection. An alternative and perhaps more straightforward explanation, however, is that FGF1-induced preservation of β-cells is primarily an indirect consequence of a reduced demand for insulin secretion (owing to normalization of glycemia). These two possibilities are not mutually exclusive, and additional studies to address them are warranted.

Our finding that sustained amelioration of hyperglycemia induced by icv FGF1 in ZDF rats occurred despite no increase of either insulin levels (over baseline values) or S_I suggests that an insulin-independent mechanism must contribute to the effect of icv FGF1 injection to increase glucose disposal. This hypothesis is strengthened by our observation that the circulating insulin level needed to normalize glycemia in icv Veh–treated ZDF rats is far higher than is observed in animals with normoglycemia induced by icv FGF1 injection.

That the brain can stimulate insulin-independent glucose disposal is well established. In rodent models of uncontrolled diabetes induced by streptozotocin, for example, hyperglycemia can be reversed by continuous icv administration of leptin, even in the face of persistent, severe insulin deficiency (10,40). Similarly, increased insulin-independent glucose disposal plays a major role in mediating the antidiabetic effect of icv FGF19 administration in *ob/ob* mice (5). Although the antidiabetic effect of icv FGF1 has been suggested to involve suppression of excessive hypothalamic-pituitary-adrenal axis activity (24), we observed no effect of icv FGF1 injection on plasma Cort levels in either the current study (in ZDF rats) or our past work (in *ob/ob* mice) (1). Excess glucagon secretion also has been hypothesized to drive diabetic hyperglycemia (41), and plasma glucagon levels were significantly decreased in ZDF rats receiving icv FGF1 compared with icv Veh. However, plasma glucagon levels do not increase in parallel with progressive hyperglycemia in ZDF rats (12), and diabetes induced by streptozotocin is not ameliorated by a glucagon-neutralizing antibody (42). On the basis of these considerations, we suspect that the modest decline in plasma glucagon is not the primary mechanism underlying the antidiabetic effect of icv FGF1.

Glucose sequestration by the liver is a major contributor to insulin-independent glucose clearance (43). After glucose enters hepatocytes through insulin-independent GLUT2, it is phosphorylated by GCK to generate glucose-6-phosphate, a rate-limiting step for HGU. Before this can occur, GCK must be dissociated from GCK regulatory protein, which otherwise sequesters the enzyme in the nucleus. Glucose-6-phosphate has several fates after conversion to triose phosphates: storage as glycogen, metabolism through the tricarboxylic acid cycle, or conversion to lactate and export from liver into the blood (14). The latter process provides the foundation for assessment of GCK activity in vivo using a mathematical model.

This model is based on the hypothesis that glucose conversion to lactate and subsequent export into the bloodstream occurs in proportion to the rate of glucose phosphorylation (and hence, GCK activity) (7). After applying this model to the dynamic relationship between plasma glucose (input to liver) and lactate (output from liver) during an FSIGT, we estimated GCK activity in animals 2 weeks after icv injection of either Veh or FGF1. We report that model-estimated liver GCK activity was effectively doubled in ZDF rats with diabetes remission induced by icv FGF1. This physiological assessment of GCK activity is in remarkable agreement with the twofold increases of both hepatic *Gck* gene expression and GCK enzymatic activity measured biochemically in liver homogenates in ZDF rats treated with icv FGF1. These data strongly suggest that increased hepatic GCK activity contributes to the mechanism underlying the sustained antidiabetic action of FGF1 in the brain, a conclusion that agrees with our earlier work showing that in *ob/ob* mice, icv FGF1 increases hepatic content of both *Gck* mRNA and glycogen while also increasing plasma lactate levels (1).

With respect to the mechanism whereby FGF1 action in the brain induces liver GCK gene expression and enzyme activity, we note that after icv FGF1 injection, cellular activation is concentrated in the mediobasal hypothalamus (1), and sympathetic connections have been identified between this brain area and liver (44). Moreover, sympathetic input to the liver appears to play a key role in controlling HGU. Specifically, studies have shown that the ability of a portal glucose load to stimulate HGU (by increasing hepatic GCK activity) is decreased by ∼75% in a canine model of T2D induced by consuming a diet high in both fat and fructose (45,46), and this effect is reversed by denervating the sympathetic supply to the liver. Sympathetic tone to the liver in this model, therefore, appears to drive the associated decrease of HGU by suppressing GCK activity. Therefore, we hypothesize that the antidiabetic action of icv FGF1 in ZDF rats involves reduced

sympathetic outflow to the liver, and additional studies are planned to test this hypothesis. We acknowledge, however, that normalization of glycemia through other mechanisms also may have contributed to increased liver GCK activity induced by icv FGF1, and additional studies are needed to address this possibility.

In conclusion, we report that in the ZDF rat model of T2D, hyperglycemia is ameliorated in a sustained manner after central FGF1 administration, consistent with our earlier work in *ob/ob* mice (1). A key difference between these two models of T2D is that in ZDF rats *1*) hyperglycemia onset is associated with progressive, severe β-cell decompensation *2*) that is not observed in *ob/ob* mice (on the C57BL/6 background). Although administration of FGF1 into the brain did not prevent this β-cell decompensation, its onset was delayed by ~3–4 weeks through mechanisms that remain to be identified. Because BG levels were normalized during this time, transient preservation of β-cell function is likely to contribute glucose lowering induced by icv FGF1. However, because plasma insulin levels in animals treated with icv FGF1 never increased over baseline values, a major role for increased GE in the sustained normalization of glycemia is implied, and our findings suggest that this increase of GE involves activation of liver GCK, which in turn increases the rate of HGU.

Acknowledgments. The authors gratefully acknowledge the technical assistance provided by Trista Harvey and Kevin Velasco at the University of Washington.

Funding. This work was supported by National Institute of Diabetes and Digestive and Kidney Diseases grants DK-114474 (J.M.S.), DK-007247 (K.M.), DK-029867 (R.N.B. and F.P.), DK-089056 (G.J.M.), DK-083042 (G.J.M. and M.W.S.), DK-035816 (G.J.M. and M.W.S.), and DK-101997 (M.W.S.). J.M.B. is supported by National Heart, Lung, and Blood Institute training grant T32-HL-007312.

Duality of Interest. Funding in support of these studies was provided to M.W.S. by Novo Nordisk (CMS-431104). No other potential conflicts of interest relevant to this article were reported.

Author Contributions. J.M.S. contributed to the experimental design, researched data, contributed to the discussion, and wrote the manuscript. K.M., J.M.B., J.M.R., M.E.M., and N.K.A. researched data and reviewed and edited the manuscript. A.S., C.I., R.J., T.H.-J., D.S., M.S., G.J.M., and M.W.S. contributed to the experimental design, researched data, contributed to the discussion, and reviewed and edited the manuscript. R.N.B., F.P., and K.J.K. contributed to the discussion and reviewed and edited the manuscript. All authors approved the final version of the manuscript. M.W.S. is the guarantor of this work and, as such, had full access to all the data in the study and takes responsibility for the integrity of the data and the accuracy of the data analysis.

Prior Presentation. Parts of this study were presented in abstract form at the 77th Scientific Sessions of the American Diabetes Association, San Diego, CA, 9–13 June 2017.

References

1. Scarlett JM, Rojas JM, Matsen ME, et al. Central injection of fibroblast growth factor 1 induces sustained remission of diabetic hyperglycemia in rodents. Nat Med 2016;22:800–806

2. Shiota M, Printz RL. Diabetes in Zucker diabetic fatty rat. Methods Mol Biol 2012;933:103–123

3. Chen C, Cohrs CM, Stertmann J, Bozsak R, Speier S. Human beta cell mass and function in diabetes: recent advances in knowledge and technologies to understand disease pathogenesis. Mol Metab 2017;6:943–957

4. Rojas JM, Matsen ME, Mundinger TO, et al. Glucose intolerance induced by blockade of central FGF receptors is linked to an acute stress response. Mol Metab 2015;4:561–568

5. Morton GJ, Matsen ME, Bracy DP, et al. FGF19 action in the brain induces insulin-independent glucose lowering. J Clin Invest 2013;123:4799–4808

6. Morton GJ, Muta K, Kaiyala KJ, et al. Evidence that the sympathetic nervous system elicits rapid, coordinated, and reciprocal adjustments of insulin secretion and insulin sensitivity during cold exposure. Diabetes 2017;66:823–834

7. Stefanovski D, Youn JH, Rees M, et al. Estimating hepatic glucokinase activity using a simple model of lactate kinetics. Diabetes Care 2012;35:1015–1020

8. Fujimoto Y, Donahue EP, Shiota M. Defect in glucokinase translocation in Zucker diabetic fatty rats. Am J Physiol Endocrinol Metab 2004;287:E414–E423

9. Paulsen SJ, Vrang N, Larsen LK, Larsen PJ, Jelsing J. Stereological assessment of pancreatic beta-cell mass development in male Zucker Diabetic Fatty (ZDF) rats: correlation with pancreatic beta-cell function. J Anat 2010;217:624–630

10. German JP, Thaler JP, Wisse BE, et al. Leptin activates a novel CNS mechanism for insulin-independent normalization of severe diabetic hyperglycemia. Endocrinology 2011;152:394–404

11. Etgen GJ, Oldham BA. Profiling of Zucker diabetic fatty rats in their progression to the overt diabetic state. Metabolism 2000;49:684–688

12. Torres TP, Catlin RL, Chan R, et al. Restoration of hepatic glucokinase expression corrects hepatic glucose flux and normalizes plasma glucose in Zucker diabetic fatty rats. Diabetes 2009;58:78–86

13. Rojas JM, Schwartz MW. Control of hepatic glucose metabolism by islet and brain. Diabetes Obes Metab 2014;16(Suppl. 1):33–40

14. Moore MC, Coate KC, Winnick JJ, An Z, Cherrington AD. Regulation of hepatic glucose uptake and storage in vivo. Adv Nutr 2012;3:286–294

15. Lovejoy J, Newby FD, Gebhart SS, DiGirolamo M. Insulin resistance in obesity is associated with elevated basal lactate levels and diminished lactate appearance following intravenous glucose and insulin. Metabolism 1992;41:22–27

16. Grayson BE, Seeley RJ, Sandoval DA. Wired on sugar: the role of the CNS in the regulation of glucose homeostasis. Nat Rev Neurosci 2013;14:24–37

17. Morton GJ, Schwartz MW. Leptin and the central nervous system control of glucose metabolism. Physiol Rev 2011;91:389–411

18. Schwartz MW, Seeley RJ, Tschöp MH, et al. Cooperation between brain and islet in glucose homeostasis and diabetes. Nature 2013;503:59–66

19. Xu J, Stanislaus S, Chinookoswong N, et al. Acute glucose-lowering and insulin-sensitizing action of FGF21 in insulin-resistant mouse models—association with liver and adipose tissue effects. Am J Physiol Endocrinol Metab 2009;297:E1105–E1114

20. Kir S, Beddow SA, Samuel VT, et al. FGF19 as a postprandial, insulin-independent activator of hepatic protein and glycogen synthesis. Science 2011;331:1621–1624

21. Kharitonenkov A, Shiyanova TL, Koester A, et al. FGF-21 as a novel metabolic regulator. J Clin Invest 2005;115:1627–1635

22. Fu L, John LM, Adams SH, et al. Fibroblast growth factor 19 increases metabolic rate and reverses dietary and leptin-deficient diabetes. Endocrinology 2004;145:2594–2603

23. Marcelin G, Jo YH, Li X, et al. Central action of FGF19 reduces hypothalamic AGRP/NPY neuron activity and improves glucose metabolism. Mol Metab 2013;3:19–28

24. Perry RJ, Lee S, Ma L, Zhang D, Schlessinger J, Shulman GI. FGF1 and FGF19 reverse diabetes by suppression of the hypothalamic-pituitary-adrenal axis. Nat Commun 2015;6:6980

25. Ryan KK, Kohli R, Gutierrez-Aguilar R, Gaitonde SG, Woods SC, Seeley RJ. Fibroblast growth factor-19 action in the brain reduces food intake and body weight and improves glucose tolerance in male rats. Endocrinology 2013;154:9–15

26. Sarruf DA, Thaler JP, Morton GJ, et al. Fibroblast growth factor 21 action in the brain increases energy expenditure and insulin sensitivity in obese rats. Diabetes 2010;59:1817–1824
27. Lan T, Morgan DA, Rahmouni K, et al. FGF19, FGF21, and an FGFR1/β-klotho-activating antibody act on the nervous system to regulate body weight and glycemia. Cell Metab 2017;26:709–718.e3
28. Lindström P. β-cell function in obese-hyperglycemic mice [*ob/ob* mice]. Adv Exp Med Biol 2010;654:463–477
29. Suh JM, Jonker JW, Ahmadian M, et al. Endocrinization of FGF1 produces a neomorphic and potent insulin sensitizer. Nature 2014;513:436–439
30. Topp BG, Atkinson LL, Finegood DT. Dynamics of insulin sensitivity, β-cell function, and β-cell mass during the development of diabetes in *fa/fa* rats. Am J Physiol Endocrinol Metab 2007;293:E1730–E1735
31. Pick A, Clark J, Kubstrup C, et al. Role of apoptosis in failure of beta-cell mass compensation for insulin resistance and beta-cell defects in the male Zucker diabetic fatty rat. Diabetes 1998;47:358–364
32. Yoshimatsu H, Niijima A, Oomura Y, Yamabe K, Katafuchi T. Effects of hypothalamic lesion on pancreatic autonomic nerve activity in the rat. Brain Res 1984;303:147–152
33. Rossi J, Santamäki P, Airaksinen MS, Herzig KH. Parasympathetic innervation and function of endocrine pancreas requires the glial cell line-derived factor family receptor α2 (GFRα2). Diabetes 2005;54:1324–1330
34. Ahrén B. Autonomic regulation of islet hormone secretion–implications for health and disease. Diabetologia 2000;43:393–410
35. Porte D Jr., Girardier L, Seydoux J, Kanazawa Y, Posternak J. Neural regulation of insulin secretion in the dog. J Clin Invest 1973;52:210–214
36. Rosario W, Singh I, Wautlet A, et al. The brain-to-pancreatic islet neuronal map reveals differential glucose regulation from distinct hypothalamic regions. Diabetes 2016;65:2711–2723
37. Kiba T, Tanaka K, Numata K, Hoshino M, Misugi K, Inoue S. Ventromedial hypothalamic lesion-induced vagal hyperactivity stimulates rat pancreatic cell proliferation. Gastroenterology 1996;110:885–893
38. Ando H, Gotoh K, Fujiwara K, et al. Glucagon-like peptide-1 reduces pancreatic β-cell mass through hypothalamic neural pathways in high-fat diet-induced obese rats. Sci Rep 2017;7:5578
39. Osundiji MA, Lam DD, Shaw J, et al. Brain glucose sensors play a significant role in the regulation of pancreatic glucose-stimulated insulin secretion. Diabetes 2012;61:321–328
40. Hidaka S, Yoshimatsu H, Kondou S, et al. Chronic central leptin infusion restores hyperglycemia independent of food intake and insulin level in streptozotocin-induced diabetic rats. FASEB J 2002;16:509–518
41. Unger RH, Cherrington AD. Glucagonocentric restructuring of diabetes: a pathophysiologic and therapeutic makeover. J Clin Invest 2012;122:4–12
42. Meek TH, Dorfman MD, Matsen ME, et al. Evidence that in uncontrolled diabetes, hyperglucagonemia is required for ketosis but not for increased hepatic glucose production or hyperglycemia. Diabetes 2015;64:2376–2387
43. Best JD, Kahn SE, Ader M, Watanabe RM, Ni TC, Bergman RN. Role of glucose effectiveness in the determination of glucose tolerance. Diabetes Care 1996;19:1018–1030
44. Uyama N, Geerts A, Reynaert H. Neural connections between the hypothalamus and the liver. Anat Rec A Discov Mol Cell Evol Biol 2004;280:808–820
45. Coate KC, Kraft G, Irimia JM, et al. Portal vein glucose entry triggers a coordinated cellular response that potentiates hepatic glucose uptake and storage in normal but not high-fat/high-fructose-fed dogs. Diabetes 2013;62:392–400
46. Dicostanzo CA, Dardevet DP, Neal DW, et al. Role of the hepatic sympathetic nerves in the regulation of net hepatic glucose uptake and the mediation of the portal glucose signal. Am J Physiol Endocrinol Metab 2006;290:E9–E16